

**Early and longitudinal microglial activation but not amyloid accumulation predict cognitive outcome in PS2APP mice**

**Carola Focke<sup>1\*</sup>, Tanja Blume<sup>1,2\*</sup>, Benedikt Zott<sup>3\*</sup>, Yuan Shi<sup>2,4\*</sup>, Maximilian Deussing<sup>1</sup>, Finn Peters<sup>4</sup>, Claudio Schmidt<sup>1</sup>, Gernot Kleinberger<sup>5,6</sup>, Simon Lindner<sup>1</sup>, Franz-Josef Gildehaus<sup>1</sup>, Leonie Beyer<sup>1</sup>, Barbara von Ungern-Sternberg<sup>1</sup>, Peter Bartenstein<sup>1,5</sup>, Laurence Ozmen<sup>7</sup>, Karlheinz Baumann<sup>7</sup>, Mario M. Dorostkar<sup>2,4</sup>, Christian Haass<sup>4,5,6</sup>, Helmuth Adelsberger<sup>3</sup>, Jochen Herms<sup>2,4,5</sup>, Axel Rominger<sup>1,5,8</sup>, Matthias Brendel<sup>1,5</sup>**

<sup>1</sup>Dept. of Nuclear Medicine, University Hospital of Munich, LMU Munich, Munich, Germany

<sup>2</sup>Center for Neuropathology and Prion Research, Ludwig-Maximilians-University of Munich, Munich, Germany

<sup>3</sup>Institute of Neuroscience, Technical University of Munich, Munich, Germany

<sup>4</sup>DZNE – German Center for Neurodegenerative Diseases, Munich, Germany

<sup>5</sup>Munich Cluster for Systems Neurology, University of Munich, Munich, Germany

<sup>6</sup>Biomedical Center (BMC), Biochemistry, Ludwig-Maximilians-Universität München, Munich, Germany

<sup>7</sup>Roche Pharma Research and Early Development, F. Hoffmann-La Roche Ltd., Basel, Switzerland

<sup>8</sup>Department of Nuclear Medicine, Inselspital, University Hospital Bern, Bern, Switzerland.

09/07/2018

\*contributed equally

**Running title:** Microglial activation rescues cognition

**Word Count:** 5276

**Corresponding author:** Dr. Matthias Brendel (resident); matthias.brendel@med.uni-muenchen.de

**First author:** Carola Focke (student); carola.focke@med.uni-muenchen.de

Shared address: Department of Nuclear Medicine, LMU Munich, Marchioninistraße 15, 81377 Munich, Germany, Phone:+49(0)89440074646/Fax:+49(0)89440077646

## **ABSTRACT**

Neuroinflammation may have beneficial or detrimental net effects on the cognitive outcome of Alzheimer's disease (AD) patients. 18kDa translocator protein (TSPO) imaging by positron-emission-tomography (PET) enables longitudinal monitoring of microglial activation *in vivo*. We compiled serial PET measures of TSPO and amyloid with terminal cognitive assessment (water maze) in an AD transgenic mouse model (PS2APP) from eight to 13 months of age, followed by immunohistochemical analyses of microglia, amyloid and synaptic density. Better cognitive outcome and higher synaptic density in PS2APP mice was predicted by higher TSPO expression at eight months. The progression of TSPO activation to 13 months also showed a moderate association with spared cognition, but amyloidosis did not correlate with the cognitive outcome, regardless of the timepoint. This first PET investigation with longitudinal TSPO- and amyloid-PET together with terminal cognitive testing in an AD mouse model indicates that continuing microglial response seems to impart preserved cognitive performance.

Key words: Amyloid-PET; TSPO-PET; synaptic density; neuroinflammation; water maze

## INTRODUCTION

Alzheimer's disease (AD) is the most common cause of dementia, and is placing an ever more onerous burden on health care due to its exponentially rising incidence with increasing age (1). Immunologically-mediated neuroinflammation is one hallmark of the pathophysiological process of AD (2,3). Current models view neuroinflammation as a double-edged sword, which can have protective or detrimental effects on brain pathology, function and the cognitive outcome (4,5). Microglia, the resident phagocytes of the innate immune system in the central nervous system continuously survey for pathogens or cellular debris, secrete factors for tissue repair and contribute to plasticity of neuronal circuits by supporting the maintenance and remodeling of synapses (6). Microglia in AD brain can recognize and phagocytose soluble and fibrillary  $\beta$ -amyloid ( $A\beta$ ), resulting in an increased inflammatory reaction (2). While this kind of acute inflammation response promotes cellular repair and restores brain integrity, chronic inflammation processes can contribute to neurodegeneration (7).

Various transgenic mouse models of AD recapitulate neuroinflammatory processes in conjunction with classical  $\beta$ -amyloid pathology (8,9); and translational studies of these models are facilitated by small animal positron-emission-tomography (PET) with radioligands for imaging of AD biomarkers (10,11). The 18kD translocator protein (TSPO), which is highly expressed at the outer mitochondrial membrane of activated microglia, presents a valuable biomarker for autoradiographic studies of microglial activation (12,13), and likewise for examination by PET of neuroinflammation in brain of AD patients or in AD mouse models (14).

PET investigation of AD patients indicated only low correlation between cerebral amyloid burden and cognitive performance (15), and  $A\beta$  deposition precedes the onset

of neuroinflammation in patients with mild cognitive impairment (16). We contend that the temporal sequences of A $\beta$  deposition and microglial activation in relation to progression of cognitive impairments is best examined through molecular imaging studies of longitudinal design. We have established this principle in serial PET examinations of A $\beta$  accumulation in PS2APP mice treated with an experimental  $\gamma$ -secretase inhibitor (17).

Given this background, we aimed now to correlate serial measures of TSPO- and  $\beta$ -amyloid-PET (A $\beta$ -PET) with the terminal cognitive assessment in the PS2APP amyloid mouse model. Our goals were as follows: (1) Assessment of possible correlations between fibrillar amyloidosis in young and aged PS2APP mice with the cognitive outcome; (2) Determine if early microglial response at baseline has an impact on the terminal cognitive outcome; (3) Determine if ongoing microglial activation influences the terminal cognitive outcome.

## **MATERIALS AND METHODS**

### **Study Design**

All experiments were performed in compliance with the National Guidelines for Animal Protection, Germany, with approval of the local animal care committee of the Government of Oberbayern (Regierung Oberbayern), and overseen by a veterinarian. The study was performed in a longitudinal design starting with dual tracer PET (TSPO and A $\beta$ ) at eight months of age as the first time-point (TP-1). Additional TSPO-PET was acquired at 9.5 months (TP-2), 11.5 months (TP-3) and 13 months (TP-4) of age, while a final A $\beta$ -PET examination was performed at TP-4. After the recovery from the last PET scan, mice were transferred to the behavioral facility and rested for one week before

initiation of the water maze (WM) tests of spatial learning. One week after behavioural test mice were deeply anaesthetized prior to transcardial perfusion. After brain extraction, we processed the brains for immunohistochemical and biochemical analyses (randomized hemispheres). Fig. 1 illustrates the study design.

Insert Fig.1

### **Animal Models and Statistical Power Analysis**

We used seven female wild-type C57Bl/6 (WT) and ten PS2APP transgenic mice (TG) in this investigation (18,19). Required sample sizes were calculated for correlation analyses (TG) and group comparisons (TG vs. WT) using G\*power (V3.1.9.2, Kiel, Germany), based on assumptions for a type I error  $\alpha=0.05$  and a power of 0.8. Effect size estimations were based on previous investigations with the same model. One additional animal was included per genotype to account for possible drop-outs.

### **PET Imaging**

*PET Acquisition, Reconstruction and Post-Processing:* All PET procedures followed an established standardized protocol for radiochemistry, acquisition and post-processing (14,20). In brief 18F-GE180 TSPO-PET ( $11.2\pm 1.5$  MBq) with an emission window of 60-90 min p.i. was used to measure cerebral TSPO expression, and 18F-florbetaben A $\beta$ -PET ( $10.8\pm 1.5$  MBq) with an emission window of 30-60 min p.i. was used for assessment of fibrillary cerebral amyloidosis. All analyses were performed by PMOD (V3.5, PMOD technologies, Basel, Switzerland). Normalization of images to standardized-uptake-value(-ratio) (SUV(R)) images was performed by the previously

validated myocardium correction method (21) for TSPO-PET and by a white matter reference region for A $\beta$ -PET (20).

*PET Image Analysis:* Standard deviation images (Z-score) were generated for all PS2APP mice for all time points and for both tracers. Here we used age-matched WT images specific (N=7 each) to calculate maps of average (AVG<sub>WT</sub>) and standard deviation (SD<sub>WT</sub>) of the relative SUVR for each tracer. Calculation of individual PS2APP Z-score images was performed by the formula (PS2APP - AVG<sub>WT</sub>)/SD<sub>WT</sub>. Voxel-wise maps for the area under the curve (AUC) of tracer uptake differences were calculated for each individual animal by generation/summation of Z-score averages between imaging time points weighted for the respective time gap. The following equations were used:

$$\text{Eq.1: TSPO-PET AUC} = 6 \cdot \frac{\text{TP1} + \text{TP2}}{2} + 8 \cdot \frac{\text{TP2} + \text{TP3}}{2} + 6 \cdot \frac{\text{TP3} + \text{TP4}}{2}$$

$$\text{Eq.2: A}\beta\text{-PET AUC} = 20 \cdot \frac{\text{TP1} + \text{TP4}}{2}$$

Voxel-wise correlation analyses of Z-score and AUC maps with behavioral results were performed by statistical parametric mapping (SPM) using SPM5 routines (Wellcome Department of Cognitive Neurology) implemented in MATLAB (version 7.1; MathWorks Inc.). For volume-of-interest (VOI)-based analyses we applied two predefined VOIs: 1) A large forebrain VOI comprising mainly neocortical and hippocampal regions with highest amyloidosis in PS2APP mice (92mm<sup>3</sup>). 2) The second VOI comprised brain areas associated with spatial learning including the hippocampal formation, piriform and entorhinal cortices as well as the amygdala (32mm<sup>3</sup>). Additionally, VOIs of peak clusters deriving from the SPM analysis were applied for extraction of individual regional Z-score values. Correlation analysis of VOI-based Z-score PET values with other modalities was performed by calculating Pearson's

coefficient of correlation.

## **Water Maze**

Mice were subjected to a modified WM task as described previously (22-24) yielding escape latency and distance to the correct platform as read outs.

Mice had to distinguish between two visible platforms, one of which was weighted in a way that it would float when the mouse climbed on (correct choice), while the other would sink (wrong choice). The correct platform was always located at the same spot in the maze, while the wrong platform as well as the site from which the mice were released into the maze was varied in a pseudorandom fashion. Visual cues on the walls of the laboratory provided orientation. Trials were terminated if the mouse had failed to reach one of the platforms within 30 sec (error of omission). In this case, or in case of a wrong choice, the experimenter placed the mouse on the correct platform. After a three-day handling period, WM training was performed on five consecutive days, with five trials per day, which were conducted 2-4 minutes apart. Memory performance was assessed by measuring the escape latency at each day of training and by the travelled distance at the last training day. For escape latency we calculated the summed average time of all trials from the start point to attaining one of the platforms. To generate as robust values as possible for individual PS2APP mice, we calculated the Z-score difference for both methods in contrast with mean WT mouse scores ( $(PS2APP - AVG_{WT}) / SD_{WT}$ ) and built a summed Z-score for each mouse. On the sixth day, the right platform was placed in the opposite quadrant of the maze to confirm that the mice had used spatial cues rather than rule-based learning to find it. Trials were filmed with a video camera and the swimming trace was extracted using custom written LabView

software (National Instruments). The experimenter was blind accordingly to the phenotype of the animals.

### **Immunohistochemistry and Biochemistry**

Immunohistochemistry in brain regions corresponding to PET was performed for fibrillar A $\beta$  (methoxy-X04), microglia (Iba1), and synaptic density (VGLUT1) as previously established (25,26). Assessment of soluble A $\beta$  assessment was performed as previously published (27).

### **Statistics**

IBM SPSS Statistics (V24.0; Chicago, IL) was used for statistical tests. Normal distribution of data was verified by the Kolmogorov-Smirnov test. Escape latency deriving from the WM test was compared between PS2APP and WT mice by a linear mixed model design including all days of training. Distance values deriving from the last day of training were compared between PS2APP and WT mice by an unpaired Student's t-test. Pearson's coefficients of correlation (R) were calculated between WM Z-Score values of PS2APP mice and their corresponding terminal Z-Scores deriving from PET (A $\beta$  and TSPO), immunohistochemistry (Iba1 and methoxy-X04) quantitation, and biochemical levels of soluble A $\beta$ . Voxel-wise and VOI based correlation analyses of baseline and serial PET measures with WM Z-Scores were conducted in SPM as described above. VGLUT1 quantification in different brain regions of PS2APP and WT mice was compared by an unpaired Student's t-test. R values were calculated for the correlation between WM Z-Score values of PS2APP mice and their corresponding

VGLUT1 quantification. A threshold of  $p < 0.05$  was deemed significant for rejection of the null hypothesis.

## **RESULTS**

### **Microglial Activity, Amyloidosis and Cognitive Performance in PS2APP Mice**

TSPO-PET examination of PS2APP mice indicated an inverted U-shape from eight to 13 months of age with peak at 11.5 months for microglial activation and A $\beta$ -PET showed the expected strong increase of amyloidosis from eight to 13 months of age (Figs. 2A and 2B). This increase was most pronounced in the frontal and parietal cortex as well as in the hippocampus and the thalamus. Microgliosis was strongest in the cortex and the hippocampus, but additionally in subcortical regions devoid of A $\beta$  like the striatum, entorhinal and piriform cortices. Behavioral testing by WM showed that PS2APP mice had cognitive impairment, as revealed by increased escape latency ( $F_{(1,15)}=35.1$ ,  $p < 0.001$ ) and +436% higher travelled distance ( $p < 0.01$ ) compared to WT mice (Fig.2C). There was no difference in speed between PS2APP and WT mice.

Insert Fig.2

### **Association of Multimodal Terminal Read Outs with Cognitive Performance**

Next, we asked if terminal read outs of PET or immunohistochemistry correlate with the cognitive performance in PS2APP mice at 13.5 months of age. The WM performance did not show any correlation with A $\beta$ -PET signal in the forebrain and in areas specifically associated with spatial learning one week earlier (both  $R < \pm 0.3$ ; Fig. 3A). On the other hand, there were trends towards better cognitive performance in mice with the highest TSPO-PET signal in forebrain ( $R = -0.46$ ,  $P = 0.18$ ; Fig. 3A) or in the areas

associated with spatial learning ( $R=-0.51$ ,  $P=0.13$ ). Immunohistochemistry confirmed *in vivo* findings: Methoxy-X04 quantification of fibrillar A $\beta$  did not indicate an association with cognitive performance ( $R<0.3$  Fig. 3A), whereas quantitation of Iba1 immunostaining showed a significant negative association between microglial activation and WM test scores ( $R=-0.77$ ,  $P=0.01$ ; Fig. 3A). Multimodal findings in representative mice with good and poor WM performance are illustrated in Figs. 3B and 3C.

Insert Fig.3

Furthermore, we saw only a weak correlation between biochemical assays of soluble A $\beta$  and cognitive performance in TG mice ( $R=-0.36$ ,  $P=0.30$ ).

### **Prediction of Cognitive Performance by Serial PET Imaging**

We undertook longitudinal *in vivo* observations of amyloidosis and microglial activity by PET to test if early or cumulative alterations over time of the pathology biomarkers predicted the cognitive outcome of PS2APP mice. We find that better cognitive performance is strongly associated with microglial activation five months earlier in forebrain ( $R=-0.71$ ,  $P<0.05$ ; Fig. 4A) and especially in cognition-associated areas ( $R=-0.82$ ,  $P<0.01$ ; Fig. 4B). Peak clusters of the amygdala, the entorhinal cortex, and the hippocampus as identified by SPM, gave especially strong regional correlations of high earlier microglial activity and better cognitive performance ( $R=-0.95$ ,  $P<0.001$ ; Fig. 4C). Statistical maps of the correlation between voxelwise microglial activity and WM performance revealed a pattern with strongest association in brain areas involved in spatial learning networks, i.e. the hippocampal formation, the thalamus, and the frontal neocortex (28) (Fig. 4D). There were no brain regions showing a negative correlation between TSPO-PET at baseline and better terminal cognitive performance.

Insert Fig.4

We had predicted an opposite relationship for cumulative TSPO-PET values over time during the whole five months imaging period, since chronic activation of microglia could damage synapses, leading to neurodegeneration (7). However, we still observed the same positive correlation, meaning that high AUCs of microglial activity were associated with a better cognitive performance (Supplemental Figs. 1A-C). Correlations between AUCs of microglial activity and WM performance were weaker when compared to TSPO-PET findings at baseline, but the spatial pattern of regions related to spatial learning networks was even better demarcated (Supplemental Fig. 1D). No brain region indicated a significant association between lower longitudinal AUCs of microglial activation and better terminal cognitive performance. There were no relevant associations of the A $\beta$ -PET signal at baseline or by longitudinal AUC analysis of amyloidosis with the terminal cognitive performance.

Finally, we asked if there is a molecular correlate of the associations between microglial activation over time and the terminal cognitive performance. Our terminal immunohistochemical analyses of synaptic density showed clear reductions of VGLUT1 in the dentate gyrus and the frontal cortex of PS2APP mice when compared to WT at 14 months of age (Fig. 5A). Reductions of VGLUT1 in individual PS2APP mice had a moderately strong correlation with behavioral assessment of cognition (Fig. 5B;  $R=-0.53$ ;  $p=0.12$  each). Even more importantly, we also observed that baseline TSPO-PET predicted synaptic density measured five months later in the dentate gyrus ( $R=0.71$ ;  $p<0.05$ ) and the frontal cortex ( $R=0.57$ ;  $p<0.1$ ; Fig. 5B and 5C). Thus, we find that an early microglial response to amyloid pathology in PS2APP TG mice protects synaptic density at follow-up.

Insert Fig.5

## DISCUSSION

This preclinical investigation exploits the advantages of serial PET for monitoring disease progression in an amyloid transgenic mouse model of AD. For the first time, we report longitudinal TSPO- and A $\beta$ -PET findings in conjunction with terminal behavioral testing and histological/biochemical examination to depict associations between longitudinal amyloidosis and neuroinflammation with cognitive outcome in an A $\beta$ /presenilin mouse model of AD. We find that high microglial activation at the onset of amyloidosis predicts for better cognitive performance in PS2APP mice at follow-up five months later, when A $\beta$  pathology is extensive. Interestingly even longitudinally persistent and terminal elevation of microglial activity were associated with a better cognitive outcome at the end of the trial. On the other hand, early and longitudinal amyloidosis did not predict cognitive outcome and terminal assessments, nor was there any association between amyloidosis and cognition. Multimodal immunohistochemical and biochemical assessments of microglia, amyloidosis and synaptic density validated and extended the *in vivo* molecular imaging results.

Neither longitudinal A $\beta$ -PET nor terminal immunohistochemistry for detection of fibrillar amyloidosis showed an association with the cognitive performance in individual PS2APP mice. Similarly, quantitative markers of  $\beta$ -amyloid had only weak correlations with cognition in aged humans (15). This seeming dissociation has been attributed to very early onset of fibrillary amyloidosis in AD, with attainment of a plateau level of amyloidosis in most patients by the time that cognitive deterioration has declared itself (29). Indeed soluble fragments of A $\beta$  might be the culprit toxic agents responsible for

synaptic damage and cognitive deterioration (30), whereas fibrillar A $\beta$  could represent an inert reservoir. Nonetheless, we did not find any correlation between terminal soluble A $\beta$  concentration in brain extracts and cognitive performance in our PS2APP mice at 14 months of age. Likewise, a recent review of different transgenic mouse models of AD did not find a significant overall correlation between soluble or insoluble levels of A $\beta$  and cognitive function (31). In this regard, the brain levels of soluble A $\beta$  may vary over time due to their dynamic turnover, which hampers the interpretation of results obtained at a single time point. We suppose that serial monitoring of soluble A $\beta$  in cerebrospinal fluid over time might reveal more meaningful relationships with the terminal cognitive outcome. The present data do not support a link between progression of amyloidosis to A $\beta$ -PET and the cognitive performance in individual PS2APP mice, which is in line with the conclusions of the aforementioned review (31).

Most importantly, we find a clear benefit of early and longitudinal microglial activation to TSPO-PET on the cognitive outcome in this cohort of PS2APP mice (Figs. 3 and 4). This finding *in vivo* was supported by immunohistochemical analysis showing that the magnitude of synaptic density loss in TG mice relative to WT was moderated by an early and ongoing microglial response. We also saw some evidence for an association between more pronounced stronger terminal neuroinflammation at 14 months and better preservation of cognitive function (Fig. 2). At first glance, our findings seem at odds with findings of neuronal dysfunction arising from exposure of neurons to pro-inflammatory mediators during chronic microglial activation (7). However, not all microglia are equal, and it remains a question about specifically what activation state of microglia an elevated TSPO-PET signal or Iba1 immunohistochemistry actually reveals. There are some hints that elevated TSPO expression is associated with a CD86-positive

pro-inflammatory microglia phenotype (32). Nonetheless, the authors of that study also observed co-localization of TSPO immunostaining with CD206-positive anti-inflammatory microglia near amyloid plaques, which could indicate microglial phagocytosis of toxic A $\beta$  (33). Clearance of accumulating debris like misfolded proteins is indeed a crucial function of anti-inflammatory microglia in their role of protecting brain tissue homeostasis (7). Interventional studies with, for example, PPAR $\gamma$  agonists to modify microglial phenotype, along with serial microglia monitoring and behavioral testing, might address this question in more detail (34). From the current data, it emerges that early microglial activation ameliorates the cognitive decline in PS2APP mice (Fig. 3). Thus, it seems an essential aspect of the innate immune system that it can respond to the developing amyloidosis caused by the genetic modification of the mouse model. The net beneficial effect of longitudinal microglial activation on cognitive function might be a matter of duration, as synapses will ultimately suffer from excessive exposure to pro-inflammatory cytokines. Thus, present protective effect of elevated microglial activity on cognitive function in PS2APP mice might have turned into deterioration at times after 14 months.

Another possible explanation for contradictory findings in studies on neuroinflammation and subsequent cognitive outcome might be attributable to differing mechanistic approaches. Most such investigations used mice with specific manipulations of genes involved in inflammatory pathways of AD and tested against WT data. We took advantage of the known phenotype heterogeneity of the PS2APP mouse (35) to study associations of biomarkers and the terminal cognitive performance in individual mice of the same genotype. Our findings imply that a strong magnitude of microglial activation is probably necessary to cope with the characteristically heavy A $\beta$  deposition in these mice

(14). This conception fits our current findings of preserved cognitive performance in mice with an early microglial response. As an explanation for this phenomenon, we invoke the recent description of two peaks of microglial activation in the time course of human sporadic AD, one occurring in the pre-symptomatic stage during early amyloid build-up and the other presenting in the dementia stage (36). Amyloid mouse models have little neuronal loss, and more closely mimic primarily pre-symptomatic and mild-cognitive-impairment stages of human AD (27). Taken together, our preclinical data support the speculation of an early protective peak of microglial activation during initial amyloid aggregation (36). Since PS2APP mice show their peak of microglial activation at approximately 11.5 months (Fig. 1), we speculate that they may lack a second peak, as they do not show much progression of neuronal loss even at very late stages >16 months of age (18).

The main strength of PET lies in its potential to monitor disease-related alterations and interventions over time in an individual. Our present findings are encouraging for longitudinal PET monitoring of microglial activation in human AD, as was recently performed with a first generation TSPO ligand (36). A longitudinal design would enable successive correlation of molecular imaging with cognitive deterioration over time. We suppose that appropriate modulation of microglial activation according to disease stage may lead to interventions with some efficacy. A second main advantage of PET lies in spatial mapping of molecular markers in the whole brain. For the first time, we have generated 3-dimensional maps of microglial activity over time in individual mice (AUC maps), and used these maps for a statistically-based voxel-wise correlation analysis with cognitive outcome parameters. Statistical testing of SPM-defined regions should be interpreted with care, but our analyses also clearly showed an enhanced

association between PET measures of microgliosis in predefined brain regions linked to spatial learning with preserved cognition (28). This methodological innovation provides the basis for designing intervention studies with endpoints relevant to human AD.

## **CONCLUSION**

Early microglial response predicts an improved cognitive outcome in PS2APP mice, whereas the magnitude of fibrillar amyloidosis in early disease stages is not predictive of cognitive performance five months later. These findings emphasize the importance of biomarkers for serial monitoring of microglial activity in AD. Furthermore, results suggest that the innate immune system could constitute a more relevant therapeutic target than amyloidosis regarding the primary objective of preserving cognitive performance.

## **ACKNOWLEDGEMENTS**

We thank Karin Bormann-Giglmaier for excellent technical assistance. Florbetaben precursor was provided by Piramal Imaging. PS2APP mice were provided by F. Hoffmann-La Roche AG. GE made GE-180 cassettes available through an early access model. We acknowledge Inglewood Biomedical Editing for manuscript editing. This work was supported by the Deutsche Forschungsgemeinschaft (DFG) by a grant to M.B.&A.R. (BR4580/1-1&RO5194/1-1) and within the framework of the Munich Cluster for Systems Neurology (EXC1010SyNergy).

## **CONFLICT OF INTEREST**

PB&AR received speaking honoraria from Piramal Imaging, LO&KB are employees of Hoffmann-La Roche, CH is an advisor of Hoffmann-La Roche. All other authors report no conflicts

## REFERENCES

1. Ziegler-Graham K, Brookmeyer R, Johnson E, Arrighi HM. Worldwide variation in the doubling time of Alzheimer's disease incidence rates. *Alzheimers Dement.* 2008;4:316-323.
2. Heneka MT, Carson MJ, El Khoury J, et al. Neuroinflammation in Alzheimer's disease. *Lancet Neurol.* 2015;14:388-405.
3. McGeer PL, McGeer EG. Mechanisms of cell death in Alzheimer disease--immunopathology. *J Neural Transm Suppl.* 1998;54:159-166.
4. Dansokho C, Heneka MT. Neuroinflammatory responses in Alzheimer's disease. *J Neural Transm (Vienna).* 2018;125:771-779.
5. Trotta T, Antonietta Panaro M, Cianciulli A, Mori G, Di Benedetto A, Porro C. Microglia-derived extracellular vesicles in Alzheimer's Disease: A double-edged sword. *Biochem Pharmacol.* 2018;148:184-192.
6. York EM, Bernier LP, MacVicar BA. Microglial modulation of neuronal activity in the healthy brain. *Dev Neurobiol.* 2018;78:593-603.
7. Heneka MT, Kummer MP, Latz E. Innate immune activation in neurodegenerative disease. *Nat Rev Immunol.* 2014;14:463-477.
8. Hall AM, Roberson ED. Mouse models of Alzheimer's disease. *Brain Res Bull.* 2012;88:3-12.
9. Teipel SJ, Buchert R, Thome J, Hampel H, Pahnke J. Development of Alzheimer-disease neuroimaging-biomarkers using mouse models with amyloid-precursor protein-transgene expression. *Prog Neurobiol.* 2011;95:547-556.
10. Zimmer ER, Leuzy A, Bhat V, Gauthier S, Rosa-Neto P. In vivo tracking of tau pathology using positron emission tomography (PET) molecular imaging in small animals. *Transl Neurodegener.* 2014;3:6.
11. Zimmer ER, Parent MJ, Cuellar AC, Gauthier S, Rosa-Neto P. MicroPET imaging and transgenic models: a blueprint for Alzheimer's disease clinical research. *Trends Neurosci.* 2014;37:629-641.
12. Cumming P, Pedersen MD, Minuzzi L, et al. Distribution of PK11195 binding sites in porcine brain studied by autoradiography in vitro and by positron emission tomography. *Synapse.* 2006;59:418-426.
13. Zimmer ER, Leuzy A, Benedet AL, Breitner J, Gauthier S, Rosa-Neto P. Tracking neuroinflammation in Alzheimer's disease: the role of positron emission tomography imaging. *J Neuroinflammation.* 2014;11:120.

14. Brendel M, Probst F, Jaworska A, et al. Glial activation and glucose metabolism in a transgenic amyloid mouse model: a triple-tracer PET study. *J Nucl Med.* 2016;57:954-960.
15. Jagust WJ, Landau SM, Shaw LM, et al. Relationships between biomarkers in aging and dementia. *Neurology.* 2009;73:1193-1199.
16. Knezevic D, Verhoeff NPL, Hafizi S, et al. Imaging microglial activation and amyloid burden in amnesic mild cognitive impairment. *J Cereb Blood Flow Metab.* 2017;271678X17741395.
17. Brendel M, Jaworska A, Herms J, et al. Amyloid-PET predicts inhibition of de novo plaque formation upon chronic gamma-secretase modulator treatment. *Mol Psychiatry.* 2015;20:1179-1187.
18. Ozmen L, Albientz A, Czech C, Jacobsen H. Expression of transgenic APP mRNA is the key determinant for beta-amyloid deposition in PS2APP transgenic mice. *Neurodegener Dis.* 2009;6:29-36.
19. Richards JG, Higgins GA, Ouagazzal AM, et al. PS2APP transgenic mice, coexpressing hPS2mut and hAPPswe, show age-related cognitive deficits associated with discrete brain amyloid deposition and inflammation. *J Neurosci.* 2003;23:8989-9003.
20. Overhoff F, Brendel M, Jaworska A, et al. Automated spatial brain normalization and hindbrain white matter reference tissue give improved [(18)F]-florbetaben PET quantitation in Alzheimer's model mice. *Front Neurosci.* 2016;10:45.
21. Deussing M, Blume T, Vomacka L, et al. Coupling between physiological TSPO expression in brain and myocardium allows stabilization of late-phase cerebral [(18)F]GE180 PET quantification. *Neuroimage.* 2017;165:83-91.
22. Sauvage M, Brabet P, Holsboer F, Bockaert J, Steckler T. Mild deficits in mice lacking pituitary adenylate cyclase-activating polypeptide receptor type 1 (PAC1) performing on memory tasks. *Brain Res Mol Brain Res.* 2000;84:79-89.
23. Busche MA, Kekus M, Adelsberger H, et al. Rescue of long-range circuit dysfunction in Alzheimer's disease models. *Nat Neurosci.* 2015;18:1623-1630.
24. Keskin AD, Kekus M, Adelsberger H, et al. BACE inhibition-dependent repair of Alzheimer's pathophysiology. *Proc Natl Acad Sci U S A.* 2017;114:8631-8636.
25. Brendel M, Focke C, Blume T, et al. Time courses of cortical glucose metabolism and microglial activity across the life span of wild-type mice: a PET study. *J Nucl Med.* 2017;58:1984-1990.
26. Dorostkar MM, Dreosti E, Odermatt B, Lagnado L. Computational processing of optical measurements of neuronal and synaptic activity in networks. *J Neurosci Methods.* 2010;188:141-150.

27. Brendel M, Kleinberger G, Probst F, et al. Increase of TREM2 during aging of an Alzheimer's disease mouse model is paralleled by microglial activation and amyloidosis. *Front Aging Neurosci.* 2017;9:8.
28. D'Hooge R, De Deyn PP. Applications of the Morris water maze in the study of learning and memory. *Brain Res Brain Res Rev.* 2001;36:60-90.
29. Jack CR, Jr., Holtzman DM. Biomarker modeling of Alzheimer's disease. *Neuron.* 2013;80:1347-1358.
30. Willem M, Tahirovic S, Busche MA, et al. eta-Secretase processing of APP inhibits neuronal activity in the hippocampus. *Nature.* 2015;526:443-447.
31. Foley AM, Ammar ZM, Lee RH, Mitchell CS. Systematic review of the relationship between amyloid-beta levels and measures of transgenic mouse cognitive deficit in Alzheimer's disease. *J Alzheimers Dis.* 2015;44:787-795.
32. Liu B, Le KX, Park MA, et al. In vivo detection of age- and disease-related increases in neuroinflammation by 18F-GE180 TSPO microPET imaging in wild-type and Alzheimer's transgenic mice. *J Neurosci.* 2015;35:15716-15730.
33. Yamanaka M, Ishikawa T, Griep A, Axt D, Kummer MP, Heneka MT. PPARgamma/RXRalpha-induced and CD36-mediated microglial amyloid-beta phagocytosis results in cognitive improvement in amyloid precursor protein/presenilin 1 mice. *J Neurosci.* 2012;32:17321-17331.
34. Zou C, Shi Y, Ohli J, Schuller U, Dorostkar MM, Herms J. Neuroinflammation impairs adaptive structural plasticity of dendritic spines in a preclinical model of Alzheimer's disease. *Acta Neuropathol.* 2016;131:235-246.
35. Brendel M, Jaworska A, Griessinger E, et al. Cross-sectional comparison of small animal [18F]-florbetaben amyloid-PET between transgenic AD mouse models. *PLoS One.* 2015;10:e0116678.
36. Fan Z, Brooks DJ, Okello A, Edison P. An early and late peak in microglial activation in Alzheimer's disease trajectory. *Brain.* 2017;140:792-803.

## Figures

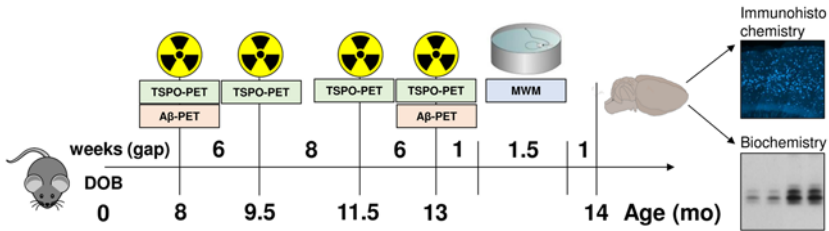


Fig.1: Schematic illustration of the study design and timeline. We obtained a series of dual tracer PET scans (TSPO and A $\beta$ ) in mice between 8 and 13 months of age. After the final scan, we administered behavioural testing by the water maze (WM), followed by transcardial perfusion with 4% paraformaldehyde and brain extraction for histochemical, immunohistochemical and biochemical analyses.

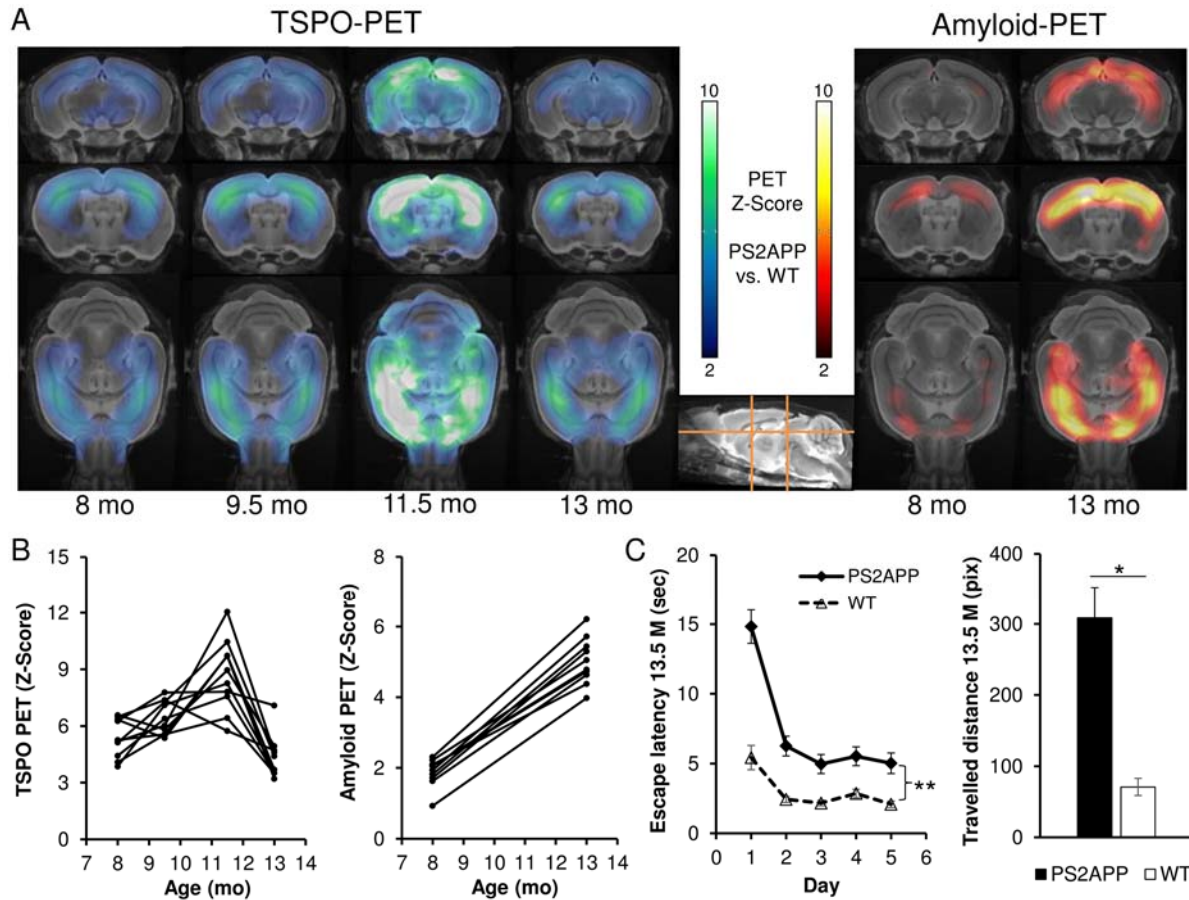


Fig.2: Longitudinal TSPO- and A $\beta$ -PET and performance in behavioural testing. (A) Cortical TSPO-PET and A $\beta$ -PET signal intensities of PS2APP mice at different ages are expressed as Z-Scores relative to findings in age-matched C57BL/6 mice. Coronal and axial slices are projected upon a T1w MRI template. (B) Progression of individual TSPO-PET Z-Scores and A $\beta$ -PET Z-Scores in the forebrain of PS2APP mice (n=10) with age. (C) Differences between PS2APP and C57Bl/6 (WT) mice for escape latency (sec) and travelled distance in pixels (pix) as water maze read outs. Error bars represent SEM. \*p<0.005; \*\*p<0.001.

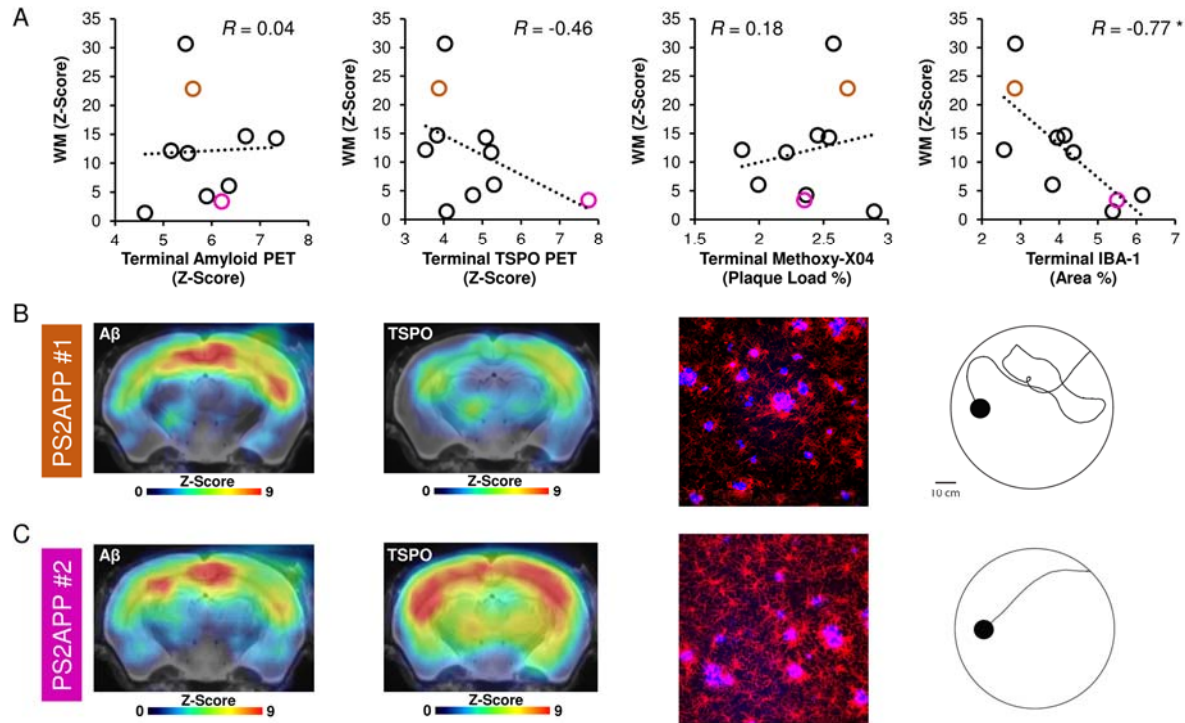


Fig.3: Multimodal correlation analysis of cognitive testing with terminal PET and immunohistochemical results in PS2APP mice at study termination. (A) Scatter plots show correlations between individual cognitive testing in the water maze task (WM, Z-score) with terminal PET and immunohistochemistry read outs. Representative PET images (Z-Score upon an MRI template), immunohistochemistry (fused methoxy-X04 (blue) and Iba1 (red)) and WM findings of individual mice, showing either low (B, orange) or high (C, magenta) markers of microglial activation at study termination. Corresponding data points in A are depicted in orange (#1, low markers of microglial activity) and magenta (#2, high markers of microglial activity). R indicates Pearson's coefficient of correlation. \* $p < 0.05$

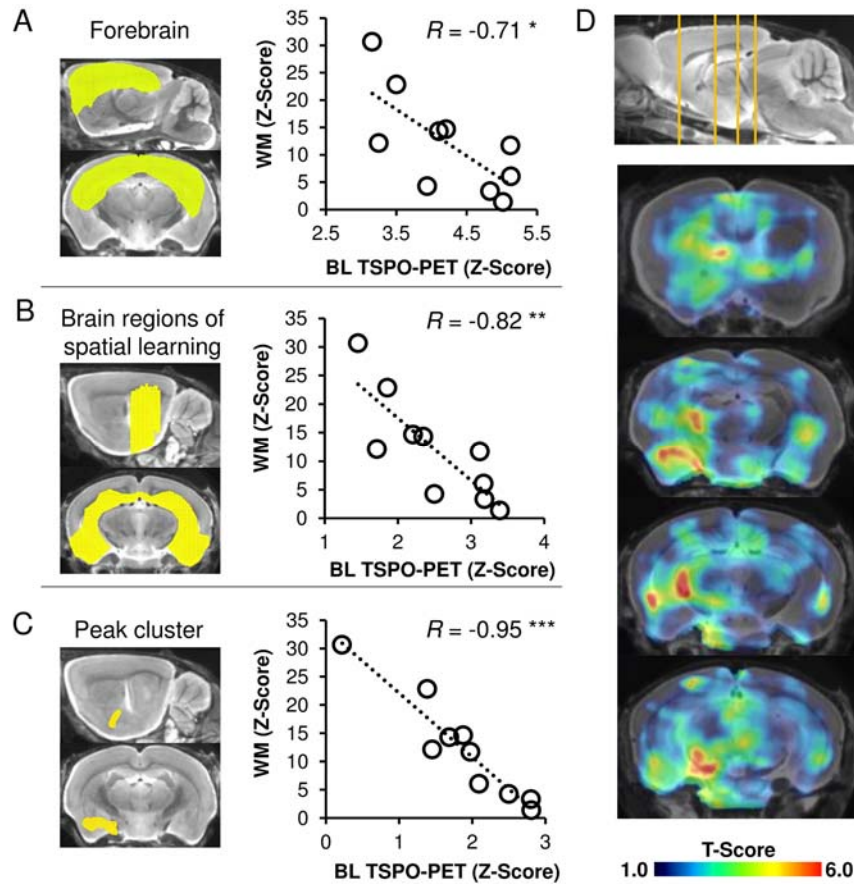


Fig.4: Prediction of cognitive performance by the magnitude of microglial activation at baseline in PS2APP mice. Correlations between individual findings in cognitive testing (Z-scores) with TSPO-PET at baseline are presented by scatter plots for (A) the forebrain, (B) brain regions associated with spatial learning, and (C) an amygdaloidal peak cluster. (D) Coronal slices depict statistical maps (T-Scores) of voxel-wise correlation between TSPO-PET at baseline and performance in water maze (WM) at study termination upon a T1w MRI template. R indicates Pearson's coefficient of correlation. \* $p < 0.05$ ; \*\* $p < 0.01$ ; \*\*\* $p < 0.001$

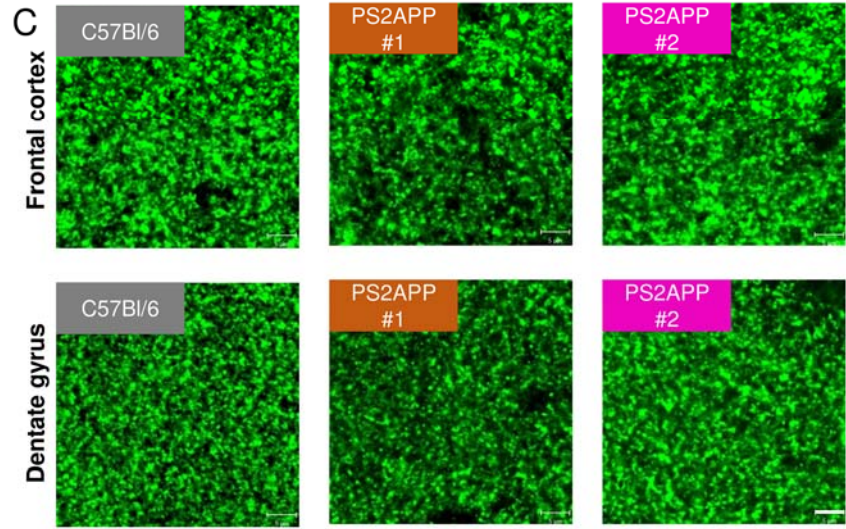
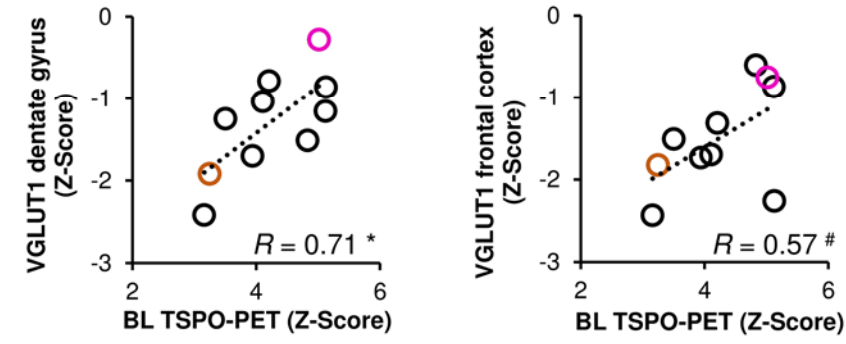
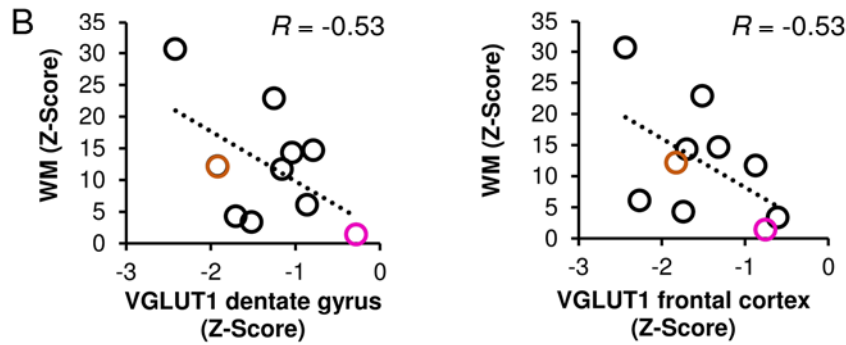
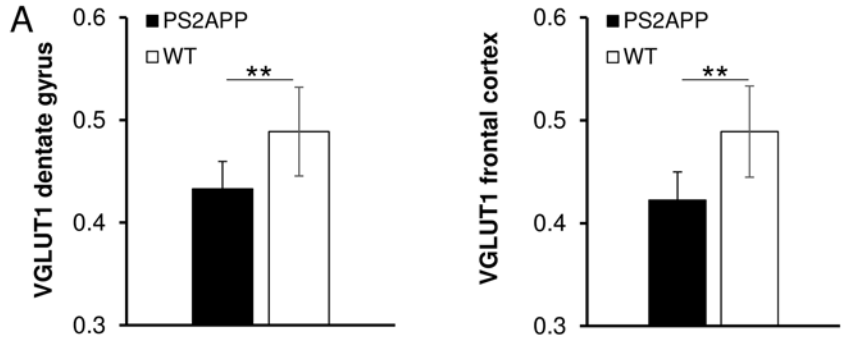
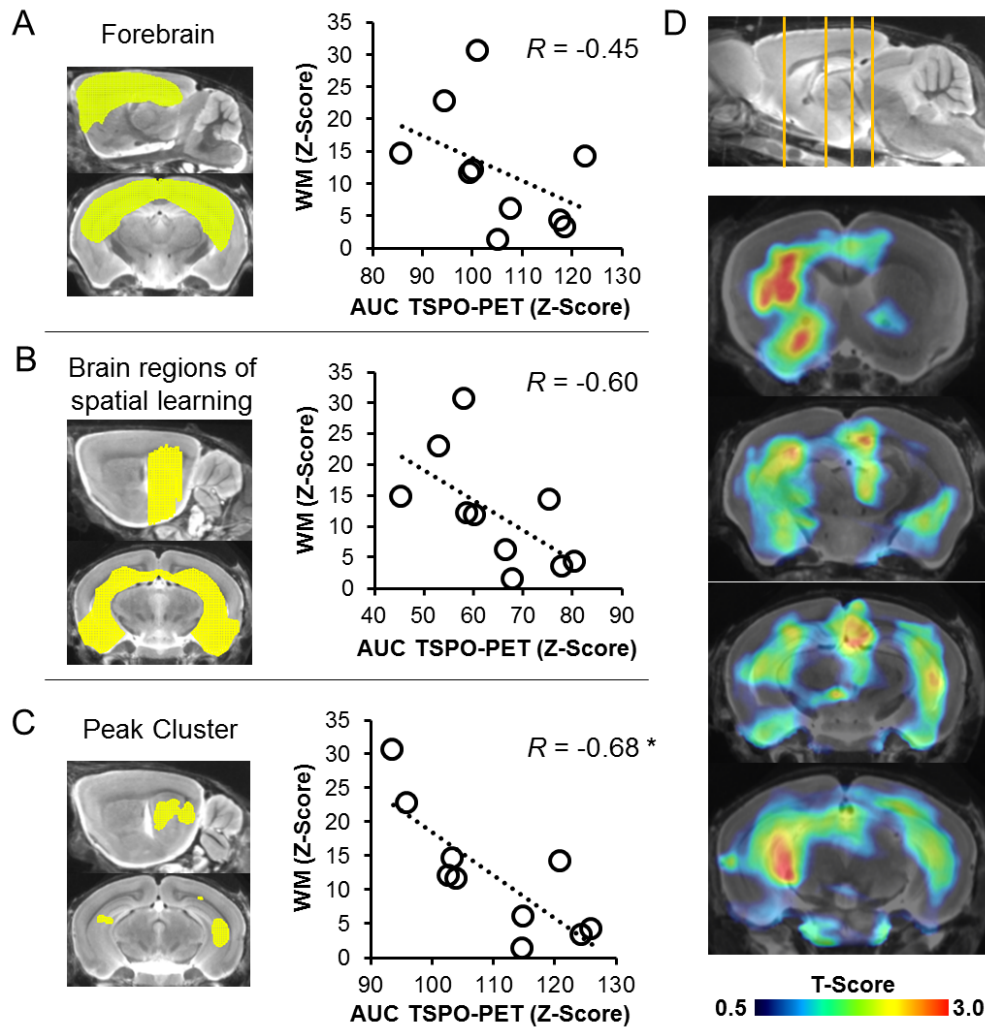


Fig.5: Moderation of the reductions of synaptic density in PS2APP mice by early microglial response. (A) Reduction in synaptic density (VGLUT1) in PS2APP mice when compared to WT. (B) Scatter plots show correlation of individual VGLUT1 alterations, cognitive testing and TSPO-PET at baseline in the dentate gyrus and the frontal cortex of PS2APP mice. (C) Findings of synaptic density (VGLUT1) in a representative C57Bl/6 WT mouse (grey), together with two PS2APP mice, one indicating severe VGLUT1 loss (#1,orange) and one indicating only minor VGLUT1 loss (#2,magenta). Corresponding data points are high-lighted in (B). R indicates Pearson's coefficient of correlation. Error bars represent SEM. # $p < 0.1$ ; \*  $p < 0.05$ . Scale bar represents 5 $\mu$ m.

## Supplemental Figure 1



**Supplemental Figure 1. Prediction of cognitive performance by the longitudinal magnitude of microglial activation in PS2APP mice.** Correlations between individual findings in cognitive testing (Z-scores) with longitudinal TSPO-PET ( $[^{18}\text{F}]\text{GE180}$ ) as expressed by the area under the curve (AUC) are presented by scatter plots for (A) the forebrain, (B) brain regions associated with spatial learning, and (C) an amygdaloidal peak cluster. (D) Coronal slices depict statistical maps (T-Scores) of voxel-wise correlation between TSPO-PET ( $[^{18}\text{F}]\text{GE180}$ ) at baseline and performance in water maze (WM) at study termination upon a T1w MRI template. R indicates Pearson's coefficient of correlation. \* $p < 0.05$